Available online at www.sciencedirect.com
SCIENCE DIRECT
Journal of Colloid and Interface Science 286 (2005) 696–709
JOURNAL OF Colloid and Interface Science
www.elsevier.com/locate/jcis

Co-solvent effects on drag reduction, rheological properties and micelle microstructures of cationic surfactants

Ying Zhang [a], Judith Schmidt [b], Yeshayahu Talmon [b], Jacques L. Zakin [a,*]

[a] *Department of Chemical Engineering, Ohio State University, Columbus, OH 43210, USA*
[b] *Department of Chemical Engineering, Technion—Israel Institute of Technology, Haifa 32000, Israel*

Received 22 March 2004; accepted 21 January 2005

Available online 19 February 2005

Abstract

Some quaternary cationic surfactants, when mixed with a counterion, are known to self-assemble into threadlike micelles in water. Such behavior causes drastic changes in rheological properties of even very dilute solutions, allowing them to be used as drag reducing agents (DRA) in turbulent pipe flow circulating systems, such as district cooling/heating systems. Surfactant self-assembly is a physicochemical phenomenon whose character depends on surfactant nature and concentration, nature of the solvent, temperature and type and concentration of counterions. This study investigates drag reduction (DR) and rheological properties of two cationic surfactants, Ethoquad O/12 (oleyl bis(hydroxyethyl)methylammonium chloride) and Ethoquad O/13 (oleyl tris(hydroxyethyl) ammonium acetate), with excess salicylate counterion (NaSal), in mixed solvents containing 0 to 28 wt% ethylene glycol (EG) and water. The addition of EG to the solvent had greater effects on solutions' DR ability, shear viscosity, apparent extensional viscosity and viscoelasticity at 25 °C than at ∼0 °C. Cryo-TEM images show threadlike micelle in these systems. DR at low temperatures in solutions containing moderate amount of EG can be utilized in a new approach to energy saving in district cooling systems using EG–water based mixtures as the cooling fluids.

Keywords: Drag reduction; Co-solvent; Cationic surfactants; Rheological properties; Threadlike micelles; Cryo-TEM

1. Introduction

District heating/cooling (DHC) systems are useful techniques for energy saving. Water is temperature-controlled in a central station and circulated through a district to heat or to cool buildings in a concentrated area, eliminating the need for individual heating or air conditioning systems in each building. A central station provides higher energy efficiency with lower cost for maintenance than the sum of many furnaces for heating or air conditioners for cooling. The elimination of these units also frees up space in the buildings, reduces local maintenance and can minimize peak electrical load periods. However, the pumping energy for water recirculation takes up about 15% of the total energy cost.

Surfactant drag reduction is a promising technology for energy saving in DHC systems [1]. Small amounts of surfactants or high polymers added to a turbulent flow significantly reduce the pressure drop over a range of turbulent flow rates. This phenomenon is called drag reduction (DR). Polymer drag reducing additives (DRA) have been applied to reduce by more than 70% the pumping energy in the transportation of hydrocarbon fluids over the past 25 years [1]. However, polymers degrade permanently in high shear regions such as pumps and contractions. Surfactant DRAs have the virtue of recovering their DR ability after mechanical degradation by self-assembling into the threadlike micelle structures responsible for DR. Their self-repairability makes surfactants more appropriate as additives for energy saving in recirculation systems such as DHC.

In conventional district cooling systems, water is cooled to about 5 °C at the outlet of a central station and returns at about 15 °C after exchanging heat with buildings in the

* Corresponding author. Fax: +1-614-292-3769.
E-mail address: zakin.1@osu.edu (J.L. Zakin).

0021-9797/$ – see front matter
doi:10.1016/j.jcis.2005.01.055

district. A new approach to energy saving is to replace the water cooling medium with 20% ethylene glycol in water (20% EG/W) solution, so that the outlet temperature can be reduced to −5 °C, doubling the temperature difference between the inlet and outlet of the distribution systems, using the same returning temperature of 15 °C. Doubling the temperature difference reduces the mass of the cooling fluid by about 50% for the same cooling capacity. By using surfactant DRAs in 20% EG/W medium, another 50% to 70% in savings on pumping energy requirements could be achieved. Accordingly, we have investigated the DR effectiveness of two cationic surfactant/counterion systems in EG/water.

Cationic quaternary ammonium salts are the most widely studied surfactant DRAs. With excess binding counterions such as salicylate (in the sodium salt, NaSal), the surfactants, at concentrations as low as a few millimoles, self-assemble into long cylindrical micelles, which can grow into giant "wormlike" or "threadlike" structures under the proper conditions. These structures undergo constant scission and recombination processes with the surfactant and counterion molecules exchanging rapidly between the states of "bound" to the micelle and "free" in the bulk solvent [2,3]. Threadlike micelles (TLMs) form in many surfactant systems and are believed to be responsible for the solutions' DR ability. In turbulent flow, the micelles are aligned along the flow direction, interacting with the growth and bursts of small turbulent eddies and vortices [4]. Cationic threadlike micelles are very sensitive to a number of factors such as the concentrations of surfactant and of counterions, their molecular structures, temperature, nature of solvent, ionic strength and shear forces.

The presence of EG in water has complicated effects on surfactant self-assembly, and therefore on their DR abilities. EG is less polar than water with a smaller degree of hydrogen bonding, and is considered to be a less efficient solvent. Ray [5] found that nonionic surfactants do form micelles even in pure EG. Sjöberg et al. [6,7] observed higher critical micelle concentration (CMC) and smaller aggregation number for cationic surfactants with increasing fractions of EG in water. Al-Sherbini et al. [8] attributed the increase in CMC of sodium dodecyl sulfate (anionic surfactant) with the addition of EG to the lower polarity, the lower dielectric constant and the larger hydrophobic surface of the co-solvent molecules. However, the effect of dielectric constant is debatable. Because the ionic strength mainly affects the interactions between surfactant headgroups, whose contribution to the free energy of micellization is negligible compared to the hydrophobic interactions of alkyl chains, Nagarajan and Wang [9,10] claimed that the low EG–hydrocarbon interfacial tension, instead of the low dielectric constant of EG, accounts for the increased CMC and decreased aggregation number. Theoretical studies of co-solvent effects on micelle formation have been mostly limited to the low surfactant concentration range, where spherical micelles form [11,12].

Only two studies of surfactant DR in co-solvent mixtures have been reported. The Gullfaks South field in the North Sea has been successful in using a zwitterionic surfactant DRA to achieve over 50% increase in the heating medium (17% EG/W) flow during a 9-month testing period [13]. Hellsten and Oskarsson [14] also showed the DR ability of zwitterionic/anionic surfactant mixtures in 5–35 wt% EG/water from 30 to 80 °C, as measured by their ability to inhibit vortex formation in a swirling flow.

Smith et al. [15] reported that cationic surfactant Ethoquad O/12 (oleyl bis(hydroxyethyl)methylammonium chloride) (EO12) with excess NaSal is DR effective in water in a wide temperature range from 2 to 80 °C. Lu [16] reported similar DR behavior of Ethoquad O/13 (oleyl tris(hydroxyethyl)ammonium acetate) (EO13). The low temperature DR effectiveness in water makes them promising candidates as effective DRAs in 20% EG/W. In this study, we investigated the effects of 0 to 28% EG on the DR ability of 5 mM EO12 solutions with excess NaSal, their rheological properties and micelle microstructures, and similarly we studied 5 mM EO13 in 0–20% EG/water.

2. Experiments

2.1. Materials

The commercial cationic surfactant, Ethoquad O12 (EO12), donated by Akzo Nobel, is a 75% active solution of oleyl bis(hydroxyethyl)methylammonium chloride in isopropyl alcohol. The sample of 50% active Ethoquad O13 (EO13), oleyl tris(hydroxyethyl) ammonium acetate, in isopropyl alcohol was also provided by Akzo Nobel. Sodium salicylate (NaSal) 99.5+% pure was purchased from Aldrich, USA and used as received. Ethylene glycol (EG) technical grade (99.5+%) was purchased from Ashland Distribution Company and used without further purification. Deuterated solvents were used for NMR experiments. Deuterated water (D_2O) 99.98% pure was purchased from Fisher Scientific. Deuterated ethylene glycol (EG-d6) 98 atom% D was purchased from C/D/N Isotopes Inc. The concentrations of EO12 and EO13 were 5 mM in all experiments and the molar ratio of NaSal to surfactant, ξ, was varied between 1 and 2.5. The appropriate amounts of active surfactant, NaSal, EG and distilled water were mixed together at room temperature and stirred for more than 6 h. All experiments were conducted after the solutions had been equilibrated for more than 24 h.

2.2. Methods

2.2.1. Surfactant drag reduction

Drag reduction was measured in a closed flow loop. The test section was a stainless tube with a length of 1.22 m and an inner diameter of 6 mm. Flow rate was measured by a Rosemount 8100 magnetic flow meter. The pressure drop

was measured by a Validyne pressure transducer. The friction factor, f, was calculated from the pressure drop and compared with the friction factor of the solvent (water or EG/W), f_s, at the same solvent Reynolds number. Drag reduction at different temperatures was calculated from the following equation over a Reynolds number range of 3×10^3 to 3×10^5:

$$\%\mathrm{DR} = \frac{f_s - f}{f_s} \times 100. \quad (1)$$

More details on the drag reduction measurements can be found in previous publications [16,17].

2.2.2. Rheological measurements

Shear viscosity was measured with a Couette cell mounted on a Rheometrics RFS II rheometer. The bob of the Couette o.d. was 32 mm, its length 24 mm, and the cup had i.d. of 34 mm. Shear viscosity at room temperature (25 °C) and low temperature (2 °C for water and −2 °C for EG/W) was measured over a shear rate range of 0.1–1000 s^{-1}.

Apparent extensional viscosity was measured with an opposing jet fluid analyzer, Rheometrics RFX. The test solution was temperature-controlled at 25 °C and at a low temperature close to 0 °C in a jacketed beaker, and sucked by two syringe pumps into two vertical tubes through a pair of opposing nozzles. The distance between the two nozzles was adjusted to be the same as their tip diameter so as to generate a symmetric flow field with a stagnant point at the center, at which the fluid was subjected to a pure extensional stress. The resistance to the pulling of the syringe pumps running at various speeds was measured by a torque transducer and translated into apparent extensional viscosity. At the same pump speed, smaller nozzle size generates higher extensional rates. Two pairs of nozzles with tip sizes of 1 and 2 mm allowed extensional viscosities to be measured from 20 to 2000 s^{-1}. All experimental results are an average of two repeated runs. Extensional viscosities measured by this method are approximate due to shear in the tubes, fluid inertia and strain history between consecutive measurements, which may affect the estimated extensional viscosity. However, RFX is an efficient method of measuring elongational viscosities of dilute fluids. It can distinguish most non-Newtonian solutions with high extensional viscosity from water. The extensional measurements in the present work are reported as apparent extensional viscosities.

First normal stress difference (N_1) was measured in a 50 mm cone-plate fixture with a cone angle of 0.04 rad, mounted on a Rheometrics RMS 800 rheometer. N_1 values at a constant shear rate were recorded as the equilibrium value. The measured readings were corrected for inertial effects according to Macosko [18] and plotted against shear rate from 20 to 1000 s^{-1}. N_1 measurements at low temperature were not possible due to a lack of temperature control for that apparatus.

2.2.3. Cryo-TEM experiments

All cryo-TEM images were taken at Technion—Israel Institute of Technology. Cryo-TEM sample preparation was conducted in a temperature-controlled chamber at 100% relative humidity. A small drop of the studied solution was applied on a perforated carbon film supported by an electron microscope grid. The drop was then blotted by a special filter paper into thin films with thickness of about 100 to 300 nm, and plunged into liquid ethane at its freezing point (∼90 K). The process was rapid enough to vitrify the liquid. The images of the vitrified sample were taken and recorded at objective lens underfocus of about 2 μm with a Philips CM120 transmission electron microscope operated at 120 kV, using an Oxford CT 3500 cooling holder operated at about −180 °C. More recent developments of the technique are described by Talmon [19].

Cryo-TEM images in 20% EG/W were taken at counterion concentrations of 7.5 mM ($\xi = 1.5$) and 12.5 mM ($\xi = 2.5$) and also at 25 and 0 °C to identify the effect of temperature on the micelle structures at rest.

2.2.4. Surface tension measurements

Surface tensions of EO12 in water and 20% EG/W at room temperature were measured in the SensaDyne bubble surface tensiometer (PC500-LV Serial #470, manufactured by SensaDyne Instrument Div., ChemDyne Research Corp., Mesa, AZ). The tensiometer uses a patented maximum differential bubble pressure method. Two probes with different orifice sizes were immersed in the test solution with nitrogen gas emerging from the tubes and thus forming bubbles in the solutions. Pressure differential between the bubbles is directly proportional to fluid surface tension. Instruments were calibrated using two standards of known surface tension values, deionized water and alcohol.

2.2.5. ^{1}H NMR experiments

^{1}H NMR experiments for the EO12 in D_2O and 20 wt% EG-d6 in D_2O systems were performed with a Bruker DRX-600 MHz (14.14 T) NMR spectrometer with a BUT 3300 digital temperature control unit at the Ohio State Campus Chemical Instrument Center. In each solvent, the ^{1}H NMR spectra for pure EO12 (5 mM) and pure NaSal (5 mM) were obtained. NaSal was added to 5 mM EO12 at the NaSal/EO12 molar ratios of 0.1, 0.2, 0.4, 0.6, 1.0, 1.5, 2.0 and 2.5. All samples were prepared in both D_2O solution and in 20% EG-d6/D_2O solution in standard NMR tubes. ^{1}H NMR spectra of all samples were obtained at 25 °C in both solvents and 2 °C in D_2O and −2 °C in EG-d6/D_2O.

3. Results and discussion

3.1. Drag reduction

Fig. 1 shows the DR properties of the system 5 mM EO12/12.5 mM NaSal in water, in which %DR was plot-

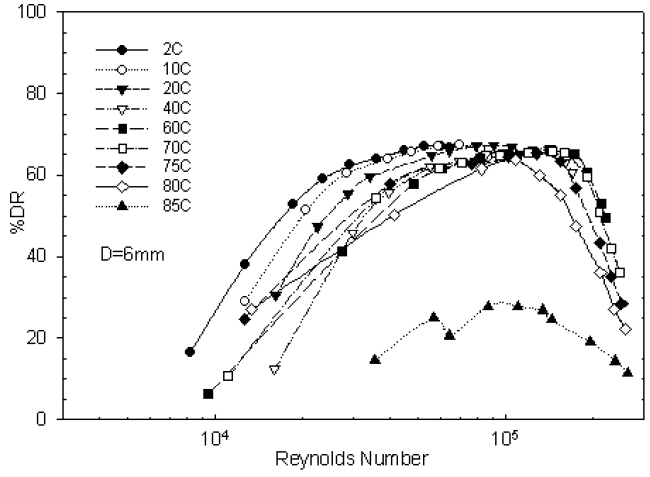

Fig. 1. DR effectiveness of 5 mM EO12/12.5 mM NaSal in water.

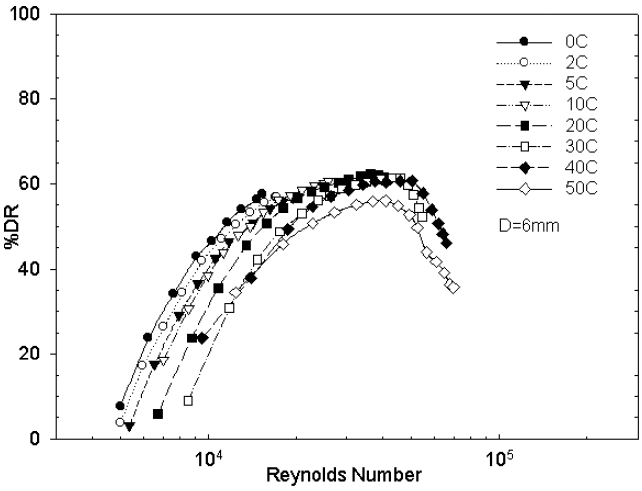

Fig. 2. DR effectiveness of 5 mM EO12/12.5 mM NaSal in 20% EG/W.

ted against Reynolds number (Re) at different temperatures. The temperature range within which the solution has a DR greater than 50% is defined as the DR effective temperature range. At each DR effective temperature tested, the %DR first increased with Re and reached a maximum. At higher flow rates, the %DR decreased with further increase in Re, presumably due to the high wall shear stresses breaking up the threadlike micelles [20]. The wall shear stress beyond which DR starts to decrease is called the critical wall shear stress (τ_{wc}). Generally, systems with long and flexible threadlike micelles have high τ_{wc}. The $\xi = 2.5$ system in water had a wide temperature range from 2 to 80 °C and DR_{max} values around 65%.

Fig. 2 shows the DR results for the system 5 mM EO12/12.5 mM NaSal in 20% EG/water, which had an upper temperature limit of 50 °C and DR_{max} values around 60%. The lowest temperature tested was 0 °C. At this temperature, when fluid viscosity was high, the maximum Re we could achieve was only 2.5×10^4, at which DR was 58% and rising.

Table 1 lists the tested DR effective temperature range, the DR_{max} at 20 °C and at a low temperature close to 0 °C, the τ_{wc} at 20 °C and at low temperature of the 5 mM EO12 solutions at different ξ values in water, 15% EG/W, 20% EG/W and 28% EG/W. For the EO13 systems, DR was measured at $\xi = 2.5$ in water and at $\xi = 1.5$ and 2.5 in 15% EG/W and in 20% EG/W. The addition of EG decreased the upper DR temperature limit of EO12 ($\xi = 2.5$) from 80 °C for the water solution to 50 °C for the 20% EG/W, and to 30 °C for the 28% EG/W. A similar decrease in the upper temperature limit for DR was observed for EO13 ($\xi = 2.5$) as 20% EG was added to water. The loss of DR at high temperature is a result of breakdown of the large threadlike micelles into shorter lengths, which is mainly caused by counterion dissociation under thermal motion [21]. The observed decrease of high temperature DR with the addition of EG indicates shorter threadlike micelles in EG solutions, which may be caused by a weaker solvophobicity and weaker counterion binding in EG–water mixtures than in pure water. However, the EG solutions are intended for low temperature use.

The low temperature limits for DR extend to below 0 °C for systems with EG addition, indicating threadlike micelles can form at sub-zero temperatures with up to 28% EG in water. This may be attributed to the good solubility of the surfactants studied, which contain two or three hydroxyethyls on the headgroup and a double bond at the mid point of its alkyl tail. Both features increase the hydrophilicity of the surfactant, which increases its solubility at low temperature. For EO12 systems, the τ_{wc} values at low temperatures decreased with EG addition. For EO13 ($\xi = 2.5$) systems, addition of 20% EG leads to a decrease in low temperature maximum %DR. Their poorer DR effectiveness in EG/W mixed solvents indicates less well developed threadlike micelles as EG concentration increased (see Section 3.3).

Increasing counterion concentration increases the upper temperature limit in both water and 20% EG/W solutions. As ξ increased from 1.5 to 2.5, the τ_{wc} values of EO12/water solutions at near 0 and at 20 °C both increased by about 35%. However, the maximum DR% at 20 °C and at low temperature did not show significant increase. The same increase in ξ led to a more than threefold increase in the low temperature τ_{wc} for the EO12/15% EG/W solution, and an increase of maximum DR% from 50 to 63 at low temperature. For the EO12/20% EG/W, EO13/15% EG/W and EO13/20% EG/W solutions, the τ_{wc} values and DR_{max} at both temperatures also increased with ξ.

Therefore, at the surfactant and counterion concentrations studied, DR threadlike micelles do form with up to 28% EG added to water but they tend to be shorter than those formed in water. The suppressive effect of EG on micelle formation in the EO12 and EO13/NaSal systems agrees with earlier observations of smaller aggregation numbers and higher CMCs for pure surfactant solutions (without counterions) in EG/W solvents [6,7].

Table 1
Summary of DR effectiveness of 5 mM Ethoquad O12 and O13/NaSal systems

Surfactant	ξ[a]	Solvent	DR temp. range, °C	$\tau_{critical}$, Pa (20 °C)	$\tau_{critical}$, Pa (low temp.)	Max %DR (20 °C)	Max %DR (low temp.)
EO12	1	Water	5 to >40	160	165	57	50
EO12	1.5	Water	<2 to >50	>120	165	66	66
EO12	2.5	Water	<2 to 80	166	220	68	68
EO12	1.5	15% EG	<−1 to >15	–	50	–	50
EO12	2.5	15% EG	<−1 to >15	–	>150	–	63
EO12	1.5	20% EG	<3 to 30	55	40	57	44
EO12	2.5	20% EG	<0 to 50	135	>115	62	60
EO12	2.5	28% EG	<−5 to 30	20	40	70	75
EO13	2.5	Water	2 to 80	135	160	70	70
EO13	1.5	15% EG	0 to >15	–	57	–	55
EO13	2.5	15% EG	<0 to >15	–	160	–	62
EO13	1.5	20% EG	0 to >15	–	63	–	51
EO13	2.5	20% EG	<−2 to 50	120	160	61	58

[a] ξ: molar ratio of NaSal to surfactant.

3.2. Rheological properties

3.2.1. Relative shear viscosities

The ratio of solution viscosity to solvent viscosity is defined as relative shear viscosity, which is mainly contributed by the microstructures. Fig. 3a shows relative shear viscosities of 5 mM EO12/12.5 mM NaSal in 0–28 wt% EG/W solutions at 25 °C. The water solution and the solutions in 15% and 20% EG/W all have similar relative shear viscosities and shear thinning behaviors at low shear rates. The viscosity of the aqueous solution shows a local increase peaking at a shear rate of 30 s^{-1}, which is caused by a shear-induced structure (SIS), resulting from the rearrangement of thread-like micelles in flow [22]. The aqueous solution also shows a second SIS peaking at a shear rate of 200 s^{-1}, with a larger viscosity increase than the previous one. The 15% and 20% EG/W both showed only one SIS peaking at a shear rate around 100 s^{-1}, with only a small increase in viscosity. The viscosity of the 28% EG/W solution has Newtonian-like behavior and is much lower than those of the lower EG concentration solutions, probably because of less effective micelle formation in this solvent. The relative shear viscosities at high shear rates (∼1000 s^{-1}) decrease with the addition of EG.

Fig. 3b shows the relative shear viscosities of EO12 (ξ = 2.5) in 0–28% EG/W solutions at a low temperature around 0 °C. The low-temperature shear viscosity of the water solution also shows two SISs (peaking at 6 and 65 s^{-1}), with a larger magnitude of viscosity increase at the low shear rate than at 25 °C (Fig. 3a). The relative shear viscosities of the 15% and 20% EG/W solutions are close to each other at both room and low temperatures, and are shear thinning with one SIS. The shear rate at which this SIS peaks at −2 °C decreases to ∼10 s^{-1}, however. While the 28% EG/W solution is Newtonian-like at 25 °C, it shows shear thinning properties at 0 °C with one SIS starting at 30 s^{-1}. The relative viscosities at high shear rates (∼1000 s^{-1}) of all solutions at low temperature also decrease with the addition of EG to the solvent.

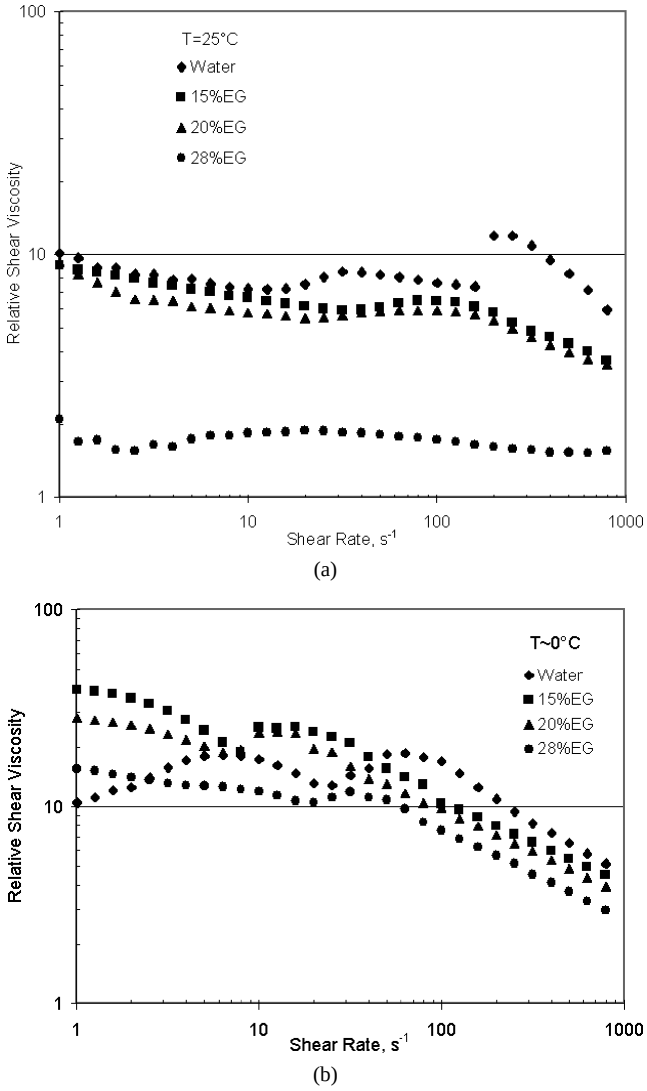

Fig. 3. Relative shear viscosity of 5 mM EO12/12.5 mM NaSal in 0–28% EG/W at (a) 25 °C and (b) at low temperature (2 °C for water and −2 °C for solutions containing EG).

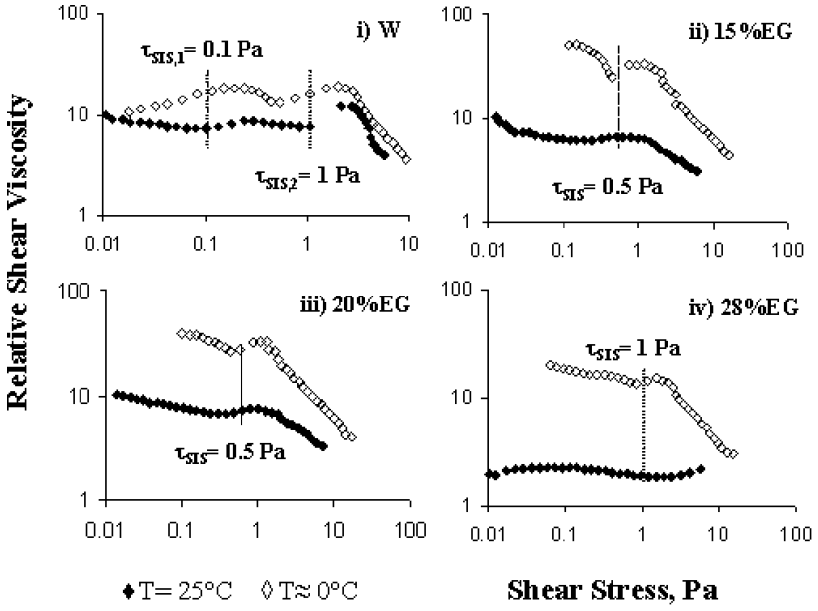

Fig. 4. Critical shear stress for SIS at room and low temperatures (5 mM EO12/12.5 mM NaSal in 0–28% EG/W).

The relative shear viscosities of EO12 solutions at room and at low temperatures are plotted against shear stress in Fig. 4. Each solution has higher relative shear viscosities at low temperature than at room temperature. While the shear rates at which SIS occurred decreases with decreasing temperature, the shear stresses for SIS are less dependent on temperature. For the EO12 ($\xi = 2.5$) water solution (Fig. 4i) which has two SISs, the first SIS corresponds to a shear stress around 0.1 Pa and the second at around 1.0 Pa for both temperatures. The 15% and 20% EG/W solutions (Figs. 4ii and 4iii) have only one SIS at both temperatures at a shear stress of about 0.5 Pa. The 28% EG/W solution (Fig. 4iv) has one SIS at around 1.0 Pa at low temperature. It did not show any SIS in the stress range measured at room temperature, possibly due to poorly developed threadlike micelle structures at this temperature. There is an upward trend at a shear stress of about 3 Pa (Fig. 4iv) but no significant rise in viscosity is observed in Fig. 3a.

These results suggest a relationship among SIS, shear stress and temperature. The addition of EG increased the shear stress for SIS to occur. While the shear rates for SIS decreased with decreasing temperature, shear stresses for SIS for the EO12 systems were insensitive to changes in temperature.

3.2.2. *Viscoelasticity*

Many DR solutions are non-Newtonian with strong viscoelasticity, indicated by high N_1, and with high ratios of extensional viscosity to shear viscosity (Θ). However, Lu et al. [23] and Lin [24] observed nonviscoelastic systems with good DR properties. While threadlike micelles are necessary for DR effectiveness, other structures such as vesicles and branched micelles in the quiescent state can transform to TLMs under shear [25–27].

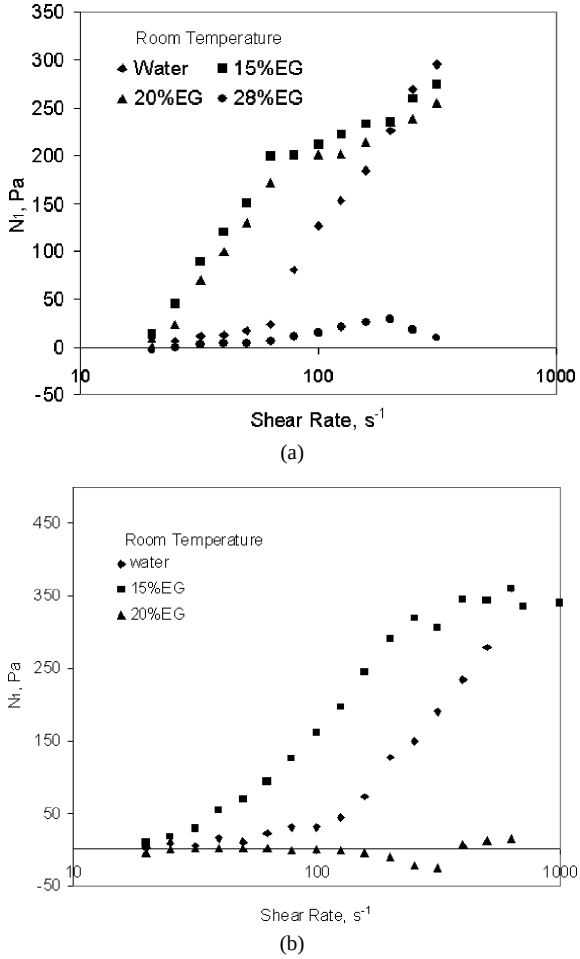

Fig. 5. N_1 of 5 mM EO12/12.5 mM NaSal (a) and 5 mM EO13/12.5 mM NaSal (b) in 0–28% EG/W at room temperature.

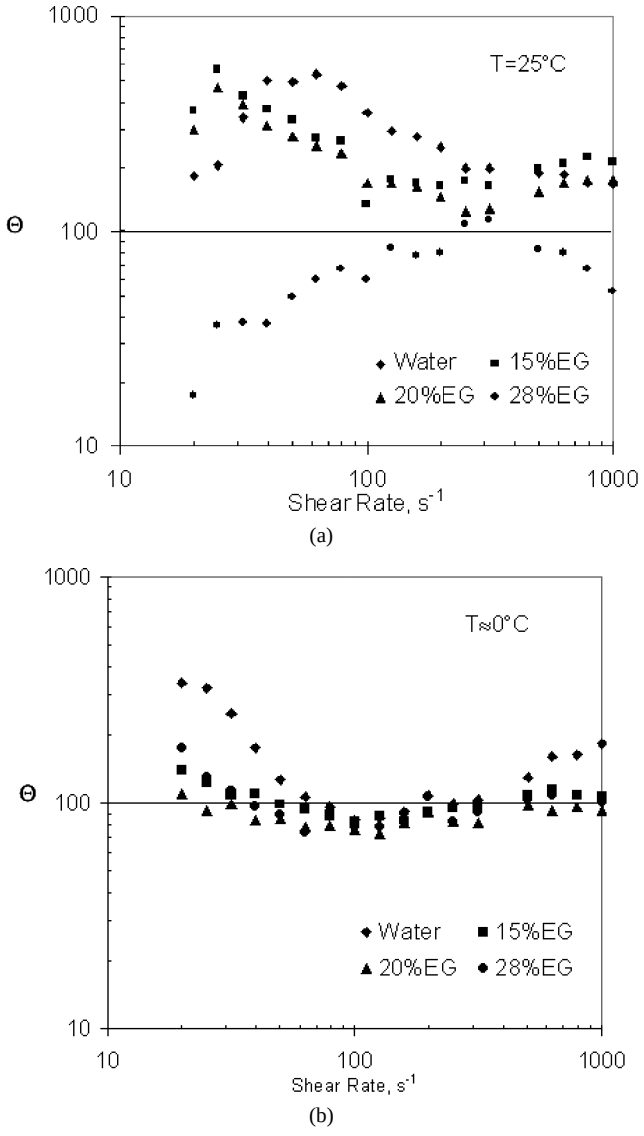

Fig. 6. Ratio of extensional viscosity to shear viscosity (Θ) of 5 mM EO12/12.5 mM NaSal in 0–28% EG/W at (a) 25 °C and (b) at low temperature (2 °C for water and −2 °C for solutions containing EG).

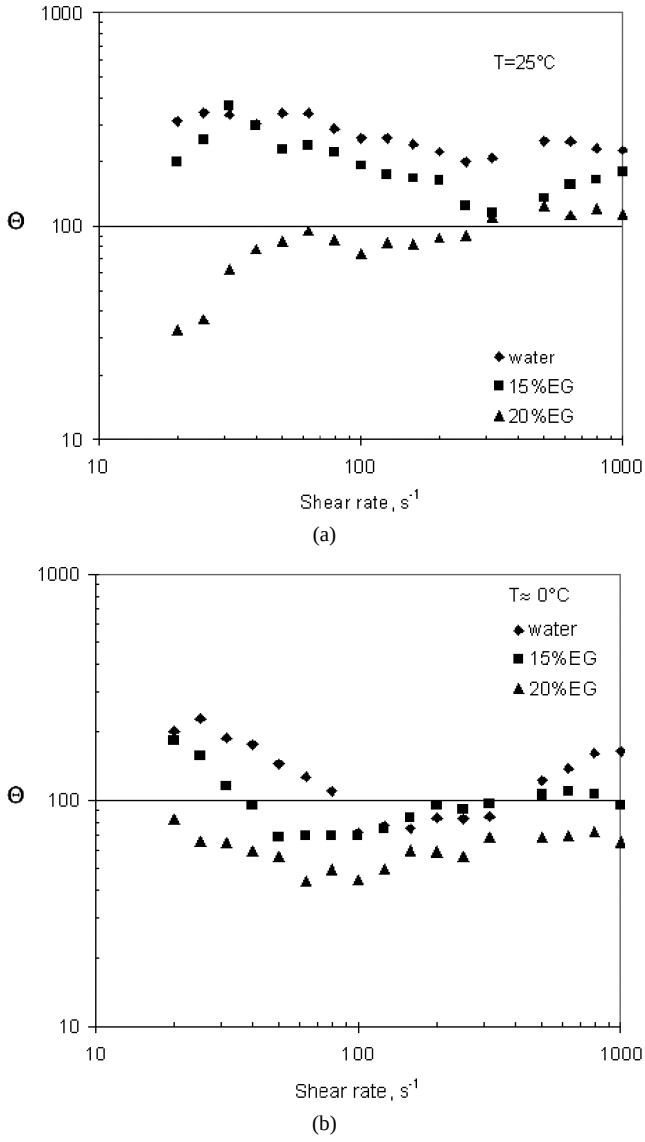

Fig. 7. Ratio of extensional viscosity to shear viscosity (Θ) of 5 mM EO13/12.5 mM NaSal in 0–20% EG/W at (a) 25 °C and (b) at low temperature (2 °C for water and −2 °C for solutions containing EG).

The first normal stress differences (N_1) of the 5 mM EO12/12.5 mM NaSal in 0–28% EG/W solutions at room temperature are shown in Fig. 5a. The 28% EG/W solution had near zero N_1 values, even though it showed modest DR at room temperature. Surprisingly, the 15% and 20% EG/W solutions had higher N_1 than the aqueous solution. Fig. 5b shows N_1 values for the EO13 ($\xi = 2.5$) systems in 0–20% EG/W. Here, again, N_1 increases as EG is added to the aqueous EO13 solution up to 15% EG/W. The 20% EG/W solution has near zero N_1 in the shear rate range tested.

Figs. 6a and 6b show the Θ values of the 5 mM EO12/12.5 mM NaSal in 0–28% EG/W solutions at 25 °C and at low temperature. At room temperature, the 0–20% EG/W solutions all have very high Θ values, which decrease with extensional/shear rate and equilibrate at a value around 200. The 28% EG/W solution has low Θ values at low rates, which increase with extensional/shear rate to a maximum of 100 at 300 s^{-1}, then decrease with further increase in the rate. At low temperature (Fig. 6b), however, all four systems with 0–28% EG show high Θ values (around 100), correlating with their effectiveness in DR. Addition of EG had less effect on the solutions Θ values at low temperature.

Figs. 7a and 7b show Θ values for the EO13 systems at 25 °C and at low temperature. At 25 °C, Θ decreases with the addition of EG. While both the water and 15% EG/W solutions have Θ values greater than 100, the Θ of 20% EG/W solution is low at low extensional rates and increases to an equilibrium value around 100 at about 70 s^{-1}. At low temperature, the Θ values are less dependent on the EG addition as shown in Fig. 7b but are generally lower than those at 25 °C. As shown by the rheological measurements, 20% EG

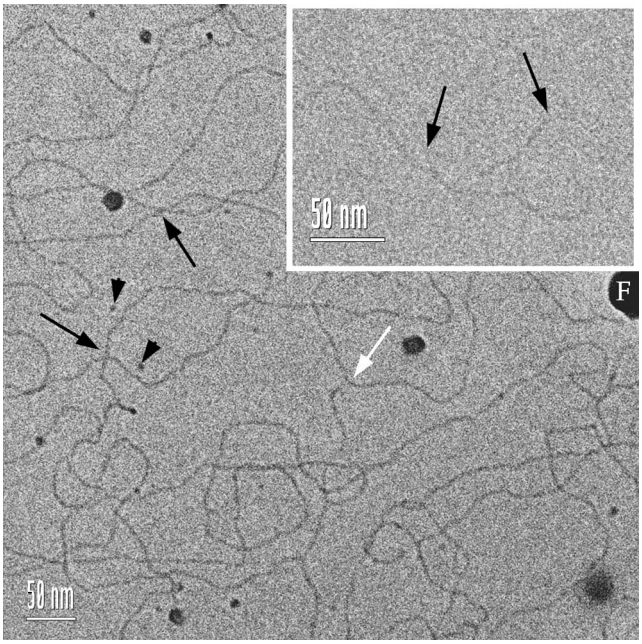

Fig. 8. Cryo-TEM images of 5 mM EO12/7.5 mM NaSal in water and in 20% EG/W (inset) at 25 °C. The arrowheads point to spherical micelles and the black arrows point to the crossover of two threadlike micelles. White arrow points to a rare branching point. The contrast in the EG solution (inset) is very weak; the micelles are indicated in the inset by black arrows.

has greater influence on the EO13 surfactant than the EO12 surfactant. The EO13 20% EG solution has rheological properties much closer to the Newtonian solvent (low relative shear viscosity (not shown here), lower N_1 and lower Θ) than the water and the EO13 15% EG/W systems, while large differences in rheological behaviors were observed for the EO12 systems only in 28% EG. Surprisingly, for both surfactants, a maximum in N_1 was observed as EG was added, although DR and other rheological properties showed monotonic decreases with EG addition.

3.3. Cryo-TEM images

Fig. 8 shows cryo-TEM images of 5 mM EO12/7.5 mM NaSal in water and in 20% EG/W at 25 °C. Long and entangled threadlike micelles are seen in the water solution coexisting with a few spherical micelles. Fewer TLMs formed in the 20% EG/W solution at this temperature. The EG/W solution gives much poorer contrast in the cryo-TEM images as seen in the inset of Fig. 8. Increasing the NaSal concentration to 12.5 mM favors micelle formation at 25 °C, both in water and in 20% EG/W, as shown in Figs. 9a and 9b. For the water solution, increase in the NaSal concentration results in much more branching in the TLMs effectively forming a network. For the 20% EG/W solution, increase in counterion concentration causes the formation of well developed TLMs with some branching points, but fewer than in the aqueous solution at the same counterion concentration and fewer loops. Note the reduced image contrast in this case too.

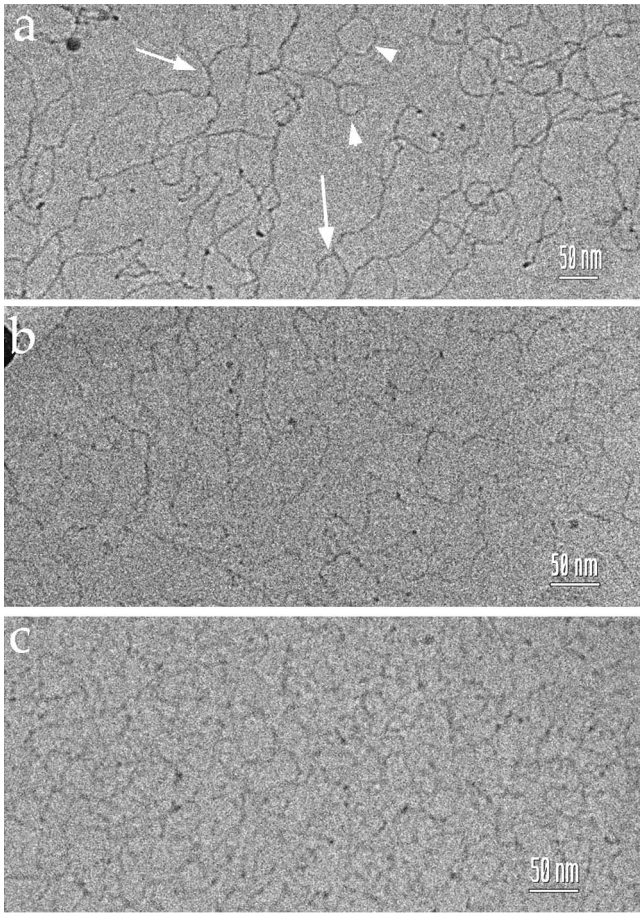

Fig. 9. (a) Cryo-TEM image of 5 mM EO12/12.5 mM NaSal in water at 25 °C. The arrows point to branching points of threadlike micelles and the arrowheads point to loops of threadlike micelles. (b) Vitrified 5 mM EO12/12.5 mM NaSal in 20% EG/W at 25 °C. Image contrast weaker. (c) Cryo-TEM image of 5 mM EO12/12.5 mM NaSal in 20% EG/W quenched from 0 °C. Threadlike micelles are better developed as compared to those at 25 °C in 20% EG/W.

Fig. 9c shows the TLMs in the 5 mM EO/12.5 mM NaSal in 20% EG/W at 0 °C. Comparing Figs. 9b and 9c, the TLMs at 0 °C seem to be better developed.

The microstructures shown by cryo-TEM suggest that addition of EG shifts the phase diagram of the surfactant system. In water, the micelles grow with the addition of counterion from cylindrical micelles coexisting with spherical ones at 7.5 mM NaSal to threadlike micelles with branched networks at 12.5 mM NaSal. Such counterion-induced micelle structure development is hampered by the addition of EG, in that micelle growth is less favored. Both $\xi = 2.5$ systems are good DRAs with the water system being higher in maximum DR, higher in τ_{wc} and has a higher upper temperature limit for effective DR. The TLMs formed in the water system at $\xi = 1.5$ are similar to those in the 20% EG/W system at $\xi = 2.5$, being long and entangled with no apparent branches or loops. The similar τ_{wc} and DR_{max} values of these two solutions at both room and low temperatures nicely show the correlations between micelle microstructures and DR. DR effectiveness for the 20% EG/W system is lower at $\xi = 1.5$

as would be expected from the cryo-TEM images. Increasing the counterion concentration to $\xi = 2.5$ promotes branching of TLMs in water. The higher τ_{wc} values and higher DR_{max} of the $\xi = 2.5$ water solution compared to the $\xi = 1.5$ water system suggest that branched TLM networks are more resistant to shear stress than dilute TLMs. This may be explained by the free movement of branching points along the cylindrical body which can release the stresses of the micelles as suggested by Appell et al. [28]. The high maximum %DR of the 28% EG/W system both at 20 °C and at low temperature is accompanied by low τ_{wc} at both temperatures and low upper temperature limit for DR. This suggests that there may be an optimum configuration of TLMs for their ability to reduce drag which is different from the optimum configuration to resist mechanical shear break-up. This would lead to a separation of DR effectiveness into the ability to depress energy dissipation, as represented by the maximum DR%, and resistance to break-up by shear stress and also by temperature rise. With excess penetrating counterions, short threads can grow into long and entangled TLMs with better DR effectiveness, but not optimum resistance to break-up under shear. Conversely, surfactant systems of branched micelle networks, while more resistant to shear degradation, do not necessarily give the highest DR%.

3.4. Surface tension results

Figs. 10a and 10b show the surface tension decreasing with increasing concentration of EO12 in water and in 20% EG/W, respectively. When the surfactant concentration is higher than a critical value, above which the surfactant molecules self-aggregate into micelles in the bulk solvents, the surface tension does not change anymore. This critical concentration for micelle formation is called CMC. Lower CMC indicates stronger self-assembling ability of a surfactant in the solvent.

Because EO12 is a mixture of oleyl bis(hydroxyethyl)-methylammonium chloride and isopropyl, the surface tension did not reach the equilibrium abruptly at the CMC, but gradually leveled off with further addition of the surfactant, as shown in Figs. 10a and 10b. However, the CMC in both solvents can be estimated by extrapolating the first-order regressions at low and high surfactant concentration ranges. The crossover concentrations of the extrapolated lines are about 3.4 mM in water and 5.4 mM in 20% EG/W. The equilibrium surface tensions in both solvents are close at about 45 dyn/cm, while the surface tension of pure water (72 dyn/cm) is higher than that of 20% EG/W (64.3 dyn/cm). Therefore, it is expected that the area per headgroup of a EO12 molecule is about the same in the two solvents. The higher estimated CMC in 20% EG/W than in water suggests weaker self-assembly in 20% EG/W than in water, which may be due to decrease in the interfacial tension between surfactant alkyl tail and the bulk solvent upon the addition of the less polar EG. This is consistent with the results of Sjöberg et al., who demonstrated that the CMC of

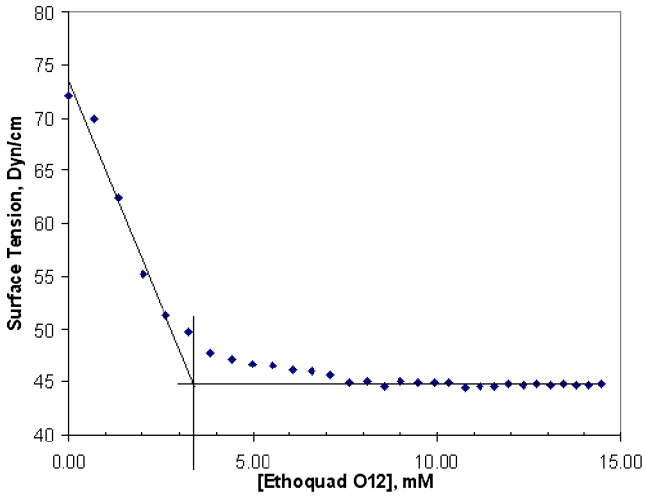

(a)

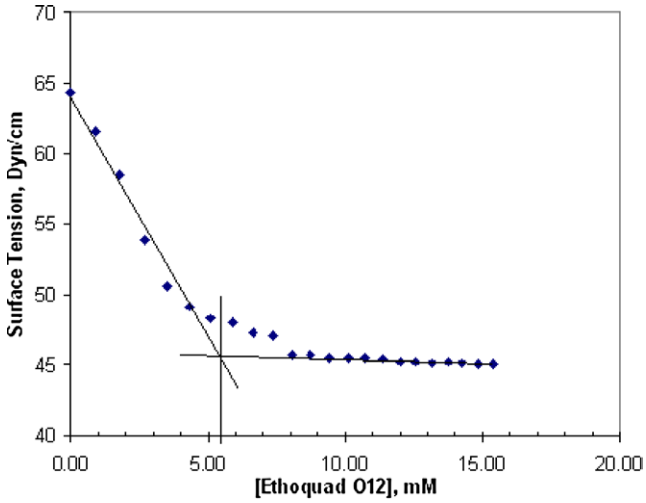

(b)

Fig. 10. Surface tension with increasing concentration of Ethoquad O12 at 25 °C in water (a) and in 20% EG/W (b).

cationic surfactant hexadecyltrimethylammonium bromide increased with the addition of EG in water [6].

3.5. ^1H NMR results

Figs. 11–14 show the ^{1}H NMR spectra of NaSal (Figs. 11 and 12) and of EO12 (Figs. 13 and 14) in the solution of 5 mM EO12 in D_2O and in 20% EG-d6/D_2O, at 25 °C (Figs. 11–14, a), 2 °C (Figs. 11 and 13, b) and −2 °C (Figs. 12 and 14, b), respectively. The bottom spectra in Figs. 11 and 12 are of 5 mM NaSal in the solvents alone, while those in Figs. 13 and 14 are of 5 mM pure EO12 in the solvents. The counterion to surfactant concentration ratio, ξ, ranged from 0.1 to 2.5 for the upper spectra (0.5 to 12.5 mM NaSal was added to 5 mM EO12 solutions). The resonance peaks of the aromatic protons on Sal– shift when Sal ions are bound to the micelles as compared to Sal– in the solvent at $\xi = \infty$. The peak identifications were determined from basic NMR principles.

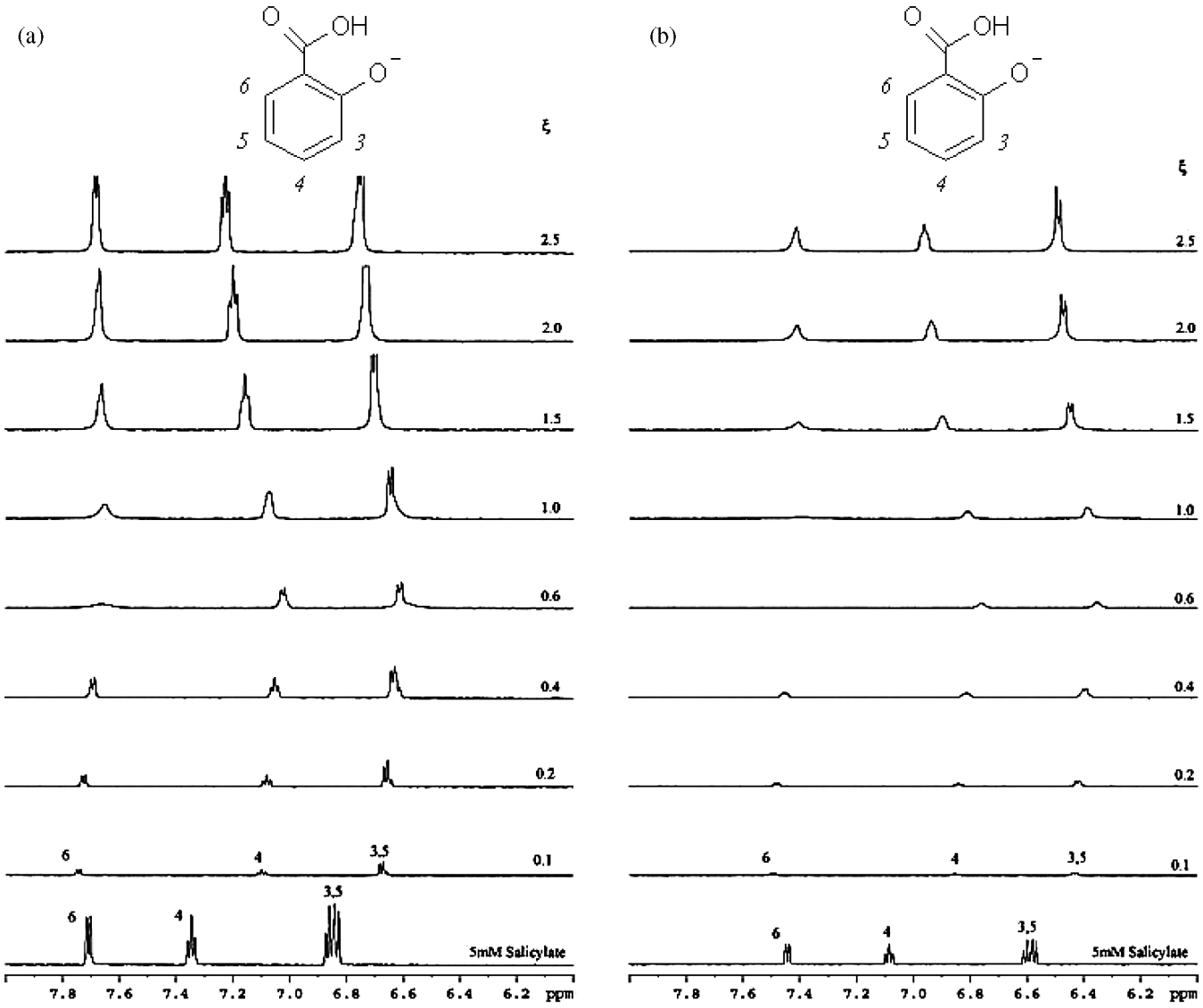

Fig. 11. ^{1}H NMR spectra of aromatic proton of salicylate in EO12/NaSal–D_2O systems at (a) 25 °C and (b) 2 °C. ξ denotes counterion to surfactant molar ratio. The bottom spectrum is 5 mM NaSal in D_2O alone. From bottom up, 0.5, 1, 2, 3, 5, 7.5, 10 and 12.5 mM NaSal was added to 5 mM EO12 solution in D_2O.

Since the exchange of Sal ions in the bound and unbound states is faster than the time scale of the NMR measurements, the observed location of the counterion proton peaks are an average of spectra peaks for the populations bound to the micelles and those in the solvent. When going from pure counterion to the $\xi = 0.1$ system, the 3-, 4- and 5-protons of the Sal ion significantly shifted upfield (lower ppm) while the 6-proton shifted downfield (higher ppm) (Figs. 11 and 12). This reflects the change in environment when the Sal ions are transferred from the bulk D_2O phase to the micelle interface with the 3-, 4- and 5-protons inserted into the less polar hydrophobic interior, while the hydrophilic $–COO^-$, –OH and the 6-proton lie in contact with solvent [29–31]. With NaSal concentration increasing to $\xi = 0.6$, only slight additional upfield shifts of 3 and 5H and 4H were detected. With further increase of counterion concentration, the 3-, 4- and 5-proton peaks begin to shift back to lower magnetic field. This is because when $\xi \geqslant 1$, the micellar surface is nearly saturated and unbound counterions are left in the bulk solvent phase as in pure NaSal solution and the peak location is an average of them.

In addition to the shifting of aromatic proton peaks in the spectra of NaSal, also observed is the resonance line broadening of EO12 with the addition of NaSal (Figs. 13 and 14). The band broadening in these systems is caused by inhibition of the end-over-end tumbling motion of threadlike micelles [29]. Micelle growth slows down the tumbling motion and longer threadlike micelles give rise to broadening. Significant band broadening occurs as ξ increases from 0.4 to 0.6 in D_2O, whereas the similar broadening in the peaks does not appear until ξ reaches 1.0 in 20% EG-d6/D_2O. Also, compared with that in water, the broad-

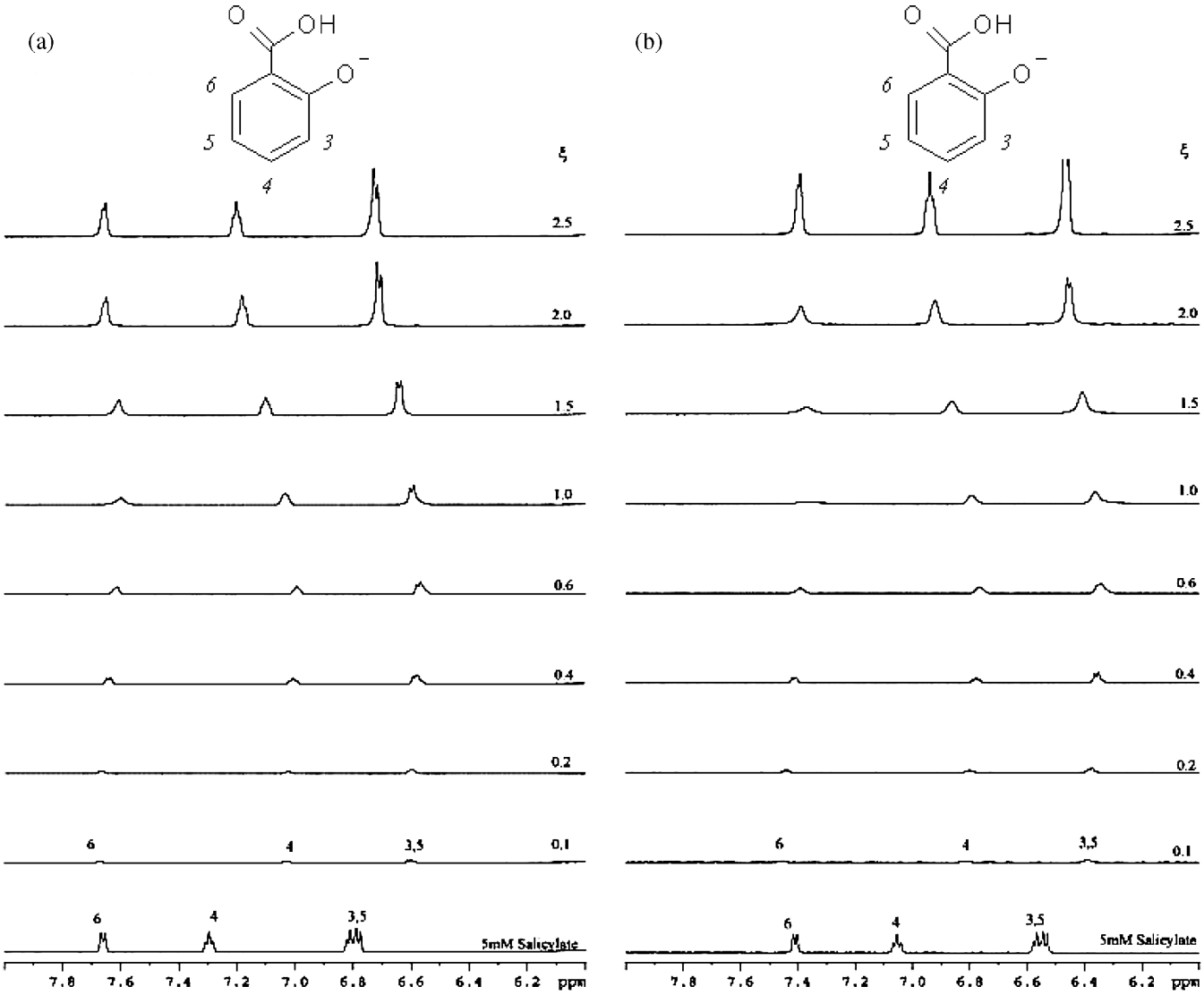

Fig. 12. ^{1}H NMR spectra of aromatic protons of salicylate in EO12/NaSal–20% EG-d6/D_2O systems at (a) 25 °C and (b) −2 °C. ξ denotes counterion to surfactant molar ratio. The bottom spectrum is 5 mM NaSal in 20% EG-d6/D_2O alone. From bottom up, 0.5, 1, 2, 3, 5, 7.5, 10 and 12.5 mM NaSal was added to 5 mM EO12 solution in 20% EG-d6/D_2O.

ening of the salicylate proton resonances is much weaker in 20% EG-d6/D_2O at room temperature, indicating smaller size of the aggregates, or shorter threadlike micelles, in the co-solvent system. However, decreasing temperature greatly enhanced the resonance broadening in the co-solvent system, as can be seen in Fig. 12b, indicating the growth of micelles as temperature decreases (see also Figs. 9a–9c). Although a similar trend was also observed in water, careful inspection of Figs. 11a and 11b shows that the role of decreasing temperature in promoting micelle growth is greater in 20% EG-d6/D_2O than in D_2O.

4. Discussion

In this study we investigated the effects of a polar nonaqueous solvent, EG, on the DR properties, rheological properties and micelle microstructures of two cationic quaternary ammonium surfactants EO12 and EO13 with excess salicylate counterions. Effective DR in such solvents at low temperatures is desired for a new approach to energy saving in district cooling systems. However, the addition of EG inhibits micelle formation as indicated by higher CMC.

Understanding the relationships among surfactant molecular structure, micellar microstructure and macroscopic behaviors would allow one to select or synthesize surfactant additives with appropriate chemical characteristics to provide desired turbulent flow properties for specific applications.

SIS has been proposed to correlate with drag reduction [32–34]. The addition of EG increased the critical shear rate for SIS in EO12 solutions but the critical shear rates were smaller at lower temperature. However, the shear stress for SIS formation was independent of temperature for each

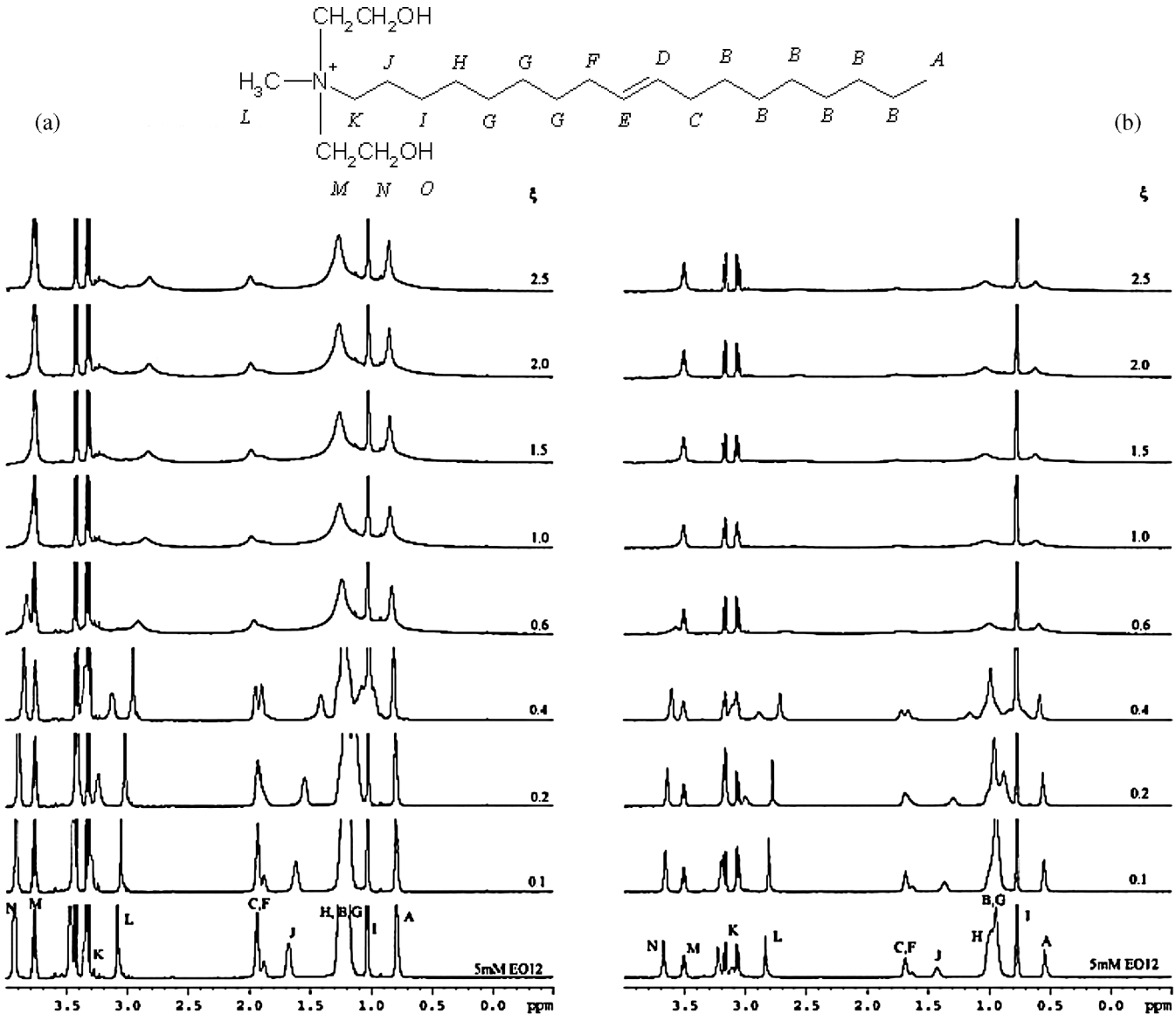

Fig. 13. ^{1}H NMR spectra of protons of EO12 in EO12/NaSal–D_2O systems at (a) 25 °C and (b) 2 °C. ξ denotes counterion to surfactant molar ratio. The bottom spectrum is 5 mM EO12 in D_2O alone. From bottom up, 0.5, 1, 2, 3, 5, 7.5, 10 and 12.5 mM NaSal was added to 5 mM EO12 solution in D_2O.

EG/water system indicating that formation of SIS is related more closely to shear stress than to shear rate. However, DR systems with no detectable SIS in the shear rate ranges tested, as in this study, have been reported [35,36], so correlation between SIS and DR is uncertain. However, it is generally believed that long, flexible threadlike or wormlike micelles resembling high polymer chains are responsible for surfactant DR. Such structures have been observed in many effective DR surfactant systems by modern cryo-TEM imaging [37]. However, unfortunately, it is not possible at the current state of the technique to obtain cryo-TEM images of microstructures in turbulent flow.

The high DR% but low τ_{wc} and low upper temperature limit for DR observed for the EO12 ($\xi = 2.5$)–28% EG/W system indicate that micelle structures in this solvent, which are most effective in reducing drag, may not sustain high shear stress and high temperature. Cryo-TEM and NMR results indicate that the size of the TLMs decreases with the addition of EG. Larger micelles and branched micellar networks have higher resistance to shear stress and can sustain higher temperatures. TLMs with shorter length give good %DR but cannot sustain high shear stresses (high Re) and dissociate at moderate wall shear stress and moderate temperature.

For the two surfactant systems studied, N_1 first increases and then drops to near zero with the addition of EG. The higher N_1 observed with modest EG addition is accompanied with a change of TLM structures with less branching, suggesting TLM networks with branching give lower solution viscoelasticity than TLMs without branching.

The effect of EG on micelle formation is also related to the surfactant chemical structure. For EO12 ($\xi = 2.5$) sys-

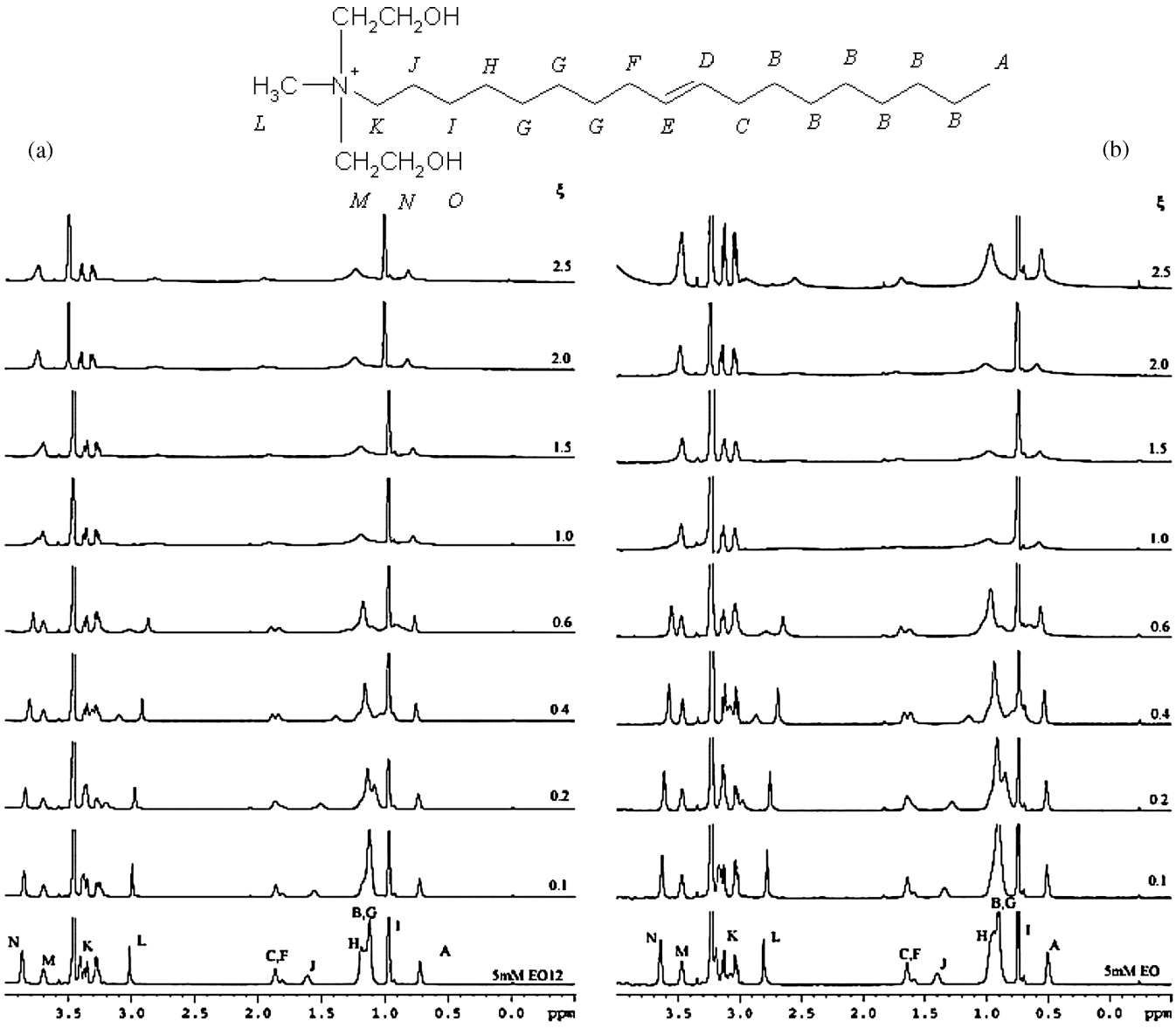

Fig. 14. ^{1}H NMR spectra of protons of EO12 in EO12/NaSal–20% EG-d6/D_2O systems at (a) 25 °C and (b) −2 °C. ξ denotes counterion to surfactant molar ratio. The bottom spectrum is 5 mM EO12 in 20% EG-d6/D_2O alone. From bottom up, 0.5, 1, 2, 3, 5, 7.5, 10 and 12.5 mM NaSal was added to 5 mM EO12 solution in 20% EG-d6/D_2O.

tems, up to 20% EG addition has only modest effect on the surfactant solutions relative shear viscosity, N_1 and Θ at room temperature, whereas addition of 28% EG caused significant decreases in the relative shear viscosity and viscoelasticity. However, in the EO13 ($\xi = 2.5$) systems, addition of EG over 15% affects N_1 and Θ at room temperature. This difference may be due to the different headgroup structures of the two surfactants. EO13 has three hydroxyethyls on the headgroup, thus the headgroup is larger and more hydrophilic than that of EO12 with two hydroxyethyls and one methyl on the headgroup. Larger headgroup favors formation of smaller (more curved) micelles. On the other hand, the headgroup hydroxyethyls can form hydrogen bonds with water molecules, and possibly with the carboxylate groups on the salicylate ions [17]. Intermicellar hydrogen bonding enhances the hydrophilic interactions of the surfactants, which favors formation of larger micelles and works against the headgroup steric effect. While the headgroup steric effect hardly changes with solvent, the strength of intermicellar H-bond is diminished with the addition of EG [38]. Thus, the micelle size of EO13 shrinks more than EO12 at the same EG content. This explains why EG addition is more effective in reducing the relative shear viscosity, N_1 and Θ of the EO13 systems compared to the EO12 systems.

5. Conclusions

In this paper, we demonstrated that DR can be achieved in 0–28% EG/W at ∼0 °C with selected cationic surfactant

DRAs. For the first time, TLM microstructures directly observed by cryo-TEM in EG/W can be well correlated with the solutions' DR, rheological properties and ^{1}H NMR spectra.

The addition of EG as a co-solvent inhibited the self-assembly of EO12 surfactant as indicated by the increase in CMC. In the surfactant solution with excess counterions, the addition of EG caused poorer development of TLMs as shown in cryo-TEM images and ^{1}H NMR results suggesting smaller micelle size. As a result, both EO12 and EO13 systems showed lower DR effectiveness in EG/W than in water, as manifested by the decrease in the upper DR temperature limit, the values of τ_{wc} and the maximum %DR. Our cryo-TEM and ^{1}H NMR results also showed that increasing counterion concentration and decreasing temperature favor micelle formation in the EG/W solvent mixtures. TLMs formed in those EG/W solvents are long enough to be DR effective and can sustain fairly high wall shear stresses at temperatures below 0 °C. The diminishing effect of EG with lowering temperature was confirmed by rheological properties of EO12 and EO13 at ∼0 °C, which are much less dependent on solvent EG fraction compared to those at 25 °C. High apparent extensional viscosity to shear viscosity ratios (Θ) are observed for all EO12 solutions, except EO12 ($\xi = 2.5$) 28% EG/water at 25 °C, and for all EO12 solutions near 0 °C. All of these solutions are DR effective. Similar behavior is observed for the EO13 solutions studied.

The shear stress at each SIS peak is independent of temperature. N_1 values at 25 °C increase with the addition of 15–10% EG, which show smaller TLMs compared to water.

Acknowledgments

This work was supported in part by the New Energy and Industrial Technology Development Organization (NEDO), Japan. Cryo-TEM was performed at the Hannah and George Krumholz Laboratory for Advanced Electron Microscopy, part of Technion Project on Complex Fluids, Microstructure and Macromolecules.

References

[1] J.L. Zakin, B. Lu, H.W. Bewersdorff, Rev. Chem. Eng. 14 (1998) 253.
[2] R. Zana, in: D.N. Rubingh, P.M. Holland (Eds.), Cationic Surfactants Physical Chemistry, vol. 37, Dekker, New York, 1991, p. 41.
[3] M.S. Turner, C. Marques, M.E. Cates, Langmuir 9 (1993) 695.
[4] P.D. Manfield, C.J. Lawrence, G.F. Hewitt, Multiphase Sci. Tech. 11 (1999) 197.
[5] A. Ray, Nature (London) 231 (1971) 313.
[6] M. Sjöberg, U. Henriksson, T. Warnheim, Langmuir 6 (1990) 1205.
[7] M. Sjöberg, M. Jansson, U. Henriksson, Langmuir 8 (1992) 409.
[8] E.A.M. Al-Sherbini, M.H. Abdel-Kader, R.Y. Hamzah, Colloids Surf. A 194 (2001) 133.
[9] R. Nagarajan, C.-C. Wang, J. Colloid Interface Sci. 178 (1996) 471.
[10] R. Nagarajan, C.-C. Wang, Langmuir 16 (2000) 5242.
[11] B.S.N.M. van Os, S. Karaborni, Recl. Trav. Chim. Pays-Bas 113 (1994) 181.
[12] R. Nagarajan, C.-C. Wang, Langmuir 11 (1995) 4673.
[13] E. Sletfjerding, A. Gladso, H. Oskarsson, S. Elsborg, in: 12th European Drag Reduction Meeting, Herning, Denmark, 2002.
[14] M. Hellsten, H. Oskarsson, International Application No. PCT/SE02/00058, August 1, 2002.
[15] B.C. Smith, L.-C. Chou, B. Lu, J.L. Zakin, in: C.A. Herb, R.K. Prud'homme (Eds.), Structure and Flow in Surfactant Solutions, in: ACS Symposium Series, vol. 578, American Chemical Society, Washington, DC, 1994, p. 370.
[16] B. Lu, Ph.D. dissertation, Ohio State University, Columbus, OH, 1997.
[17] L.-C. Chou, Ph.D. dissertation, Ohio State University, Columbus, OH, 1991.
[18] C.W. Macosko, Rheology: Principles, Measurements, and Applications, Wiley–VCH, New York, 1994.
[19] Y. Talmon, in: B.P. Binks (Ed.), Modern Characterization Methods of Surfactant Systems, in: Surfactant Science Series, vol. 83, Dekker, 1999, p. 147.
[20] Y. Qi, Y. Kawaguchi, R.N. Christensen, J.L. Zakin, Int. J. Heat Mass Transfer 46 (2003) 5161.
[21] D.E. Evans, D.D. Miller, in: S.E. Friberg, B. Lindman (Eds.), Organized Solutions, in: Surfactant Science Series, vol. 44, Dekker, New York, 1992, p. 33.
[22] (a) H. Rehage, H. Hoffmann, Rheol. Acta 21 (1982) 561;
(b) V.K. Jindal, J. Kalus, H. Pilsl, H. Hoffmann, P. Lindner, J. Phys. Chem. 94 (1990) 3129;
(c) V. Schmitt, F. Schosseler, F. Lequeux, Europhys. Lett. 30 (1995) 31;
(d) R. Oda, P. Panizza, M. Schmutz, F. Lequeux, Langmuir 13 (1997) 6407;
(e) J.-F. Berret, R. Gamez-Corrales, J. Oberdisse, L.M. Walker, P. Lindner, Europhys. Lett. 41 (1998) 677;
(f) W. Richtering, Curr. Opin. Colloid Interface Sci. 6 (2001) 446;
(g) M.T. Truong, L.M. Walker, Langmuir 18 (2002) 2024.
[23] B. Lu, X. Li, J.L. Zakin, Y. Talmon, J. Non-Newtonian Fluid Mech. 71 (1997) 59.
[24] Z. Lin, Ph.D. dissertation, Ohio State University, Columbus, OH, 2000.
[25] E. Mendes, J. Narayanan, R. Oda, F. Kern, S.J. Candau, J. Phys. Chem. B 101 (1997) 2256.
[26] Y. Zheng, Z. Lin, J.L. Zakin, Y. Talmon, H.T. Davis, L.E. Scriven, J. Phys. Chem. B 104 (2000) 5263.
[27] Z. Lin, Y. Zheng, H.T. Davis, L.E. Scriven, Y. Talmon, J.L. Zakin, J. Rheol. 45 (2001) 963.
[28] J. Appell, G. Porte, A. Khatory, F. Kern, S.J. Candau, J. Phys. II 2 (1992) 1045.
[29] U. Olsson, O. Söderman, P.J. Guéring, Phys. Chem. 90 (1986) 5223.
[30] T. Shikata, H. Hirata, T. Kotaka, Langmuir 4 (1988) 354.
[31] B.C. Smith, L.-C. Chou, J.L. Zakin, J. Rheol. 38 (1994) 73.
[32] C. Liu, D.J. Pine, Phys. Rev. Lett. 77 (1996) 2121.
[33] S. Koch, Rheol. Acta 36 (1997) 639.
[34] S. Hoffman, H. Hoffman, J. Phys. Chem. B 102 (1998) 5614.
[35] J. Myska, P. Stern, Colloid Polym. Sci. 276 (1998) 816.
[36] Y. Qi, J.L. Zakin, Ind. Eng. Chem. Res. 41 (2002) 6326.
[37] B. Lu, X. Li, L.E. Scriven, H.T. Davis, Y. Talmon, J.L. Zakin, Langmuir 14 (1998) 8.
[38] Y. Koga, J. Solution Chem. 32 (2003) 803.